J Neurophysiol 106: 849–859, 2011.
First published May 25, 2011; doi:10.1152/jn.00559.2010.

Fine frequency tuning in monkey auditory cortex and thalamus

Edward L. Bartlett,[1]* Srivatsun Sadagopan,[1,2]* and Xiaoqin Wang[1]
[1]*Department of Biomedical Engineering, and* [2]*Department of Neuroscience, Johns Hopkins University, Baltimore, Maryland*

Submitted 23 June 2010; accepted in final form 23 May 2011

Bartlett EL, Sadagopan S, Wang X. Fine frequency tuning in monkey auditory cortex and thalamus. *J Neurophysiol* 106: 849–859, 2011. First published May 25, 2011; doi:10.1152/jn.00559.2010.— The frequency resolution of neurons throughout the ascending auditory pathway is important for understanding how sounds are processed. In many animal studies, the frequency tuning widths are about 1/5th octave wide in auditory nerve fibers and much wider in auditory cortex neurons. Psychophysical studies show that humans are capable of discriminating far finer frequency differences. A recent study suggested that this is perhaps attributable to fine frequency tuning of neurons in human auditory cortex (Bitterman Y, Mukamel R, Malach R, Fried I, Nelken I. *Nature* 451: 197–201, 2008). We investigated whether such fine frequency tuning was restricted to human auditory cortex by examining the frequency tuning width in the awake common marmoset monkey. We show that 27% of neurons in the primary auditory cortex exhibit frequency tuning that is finer than the typical frequency tuning of the auditory nerve and substantially finer than previously reported cortical data obtained from anesthetized animals. Fine frequency tuning is also present in 76% of neurons of the auditory thalamus in awake marmosets. Frequency tuning was narrower during the sustained response compared to the onset response in auditory cortex neurons but not in thalamic neurons, suggesting that thalamocortical or intracortical dynamics shape time-dependent frequency tuning in cortex. These findings challenge the notion that the fine frequency tuning of auditory cortex is unique to human auditory cortex and that it is a de novo cortical property, suggesting that the broader tuning observed in previous animal studies may arise from the use of anesthesia during physiological recordings or from species differences.

medial geniculate; thalamocortical dynamics; bandwidth; marmoset

FINE-GRAINED REPRESENTATION of sound frequency is critical for sound segregation and recognition (Bregman 1990, p. 58–68, 83–92, 642–654; Carlyon 1992; Micheyl and Oxenham 2010). The initial stages of auditory processing decompose sound signals into frequency bands that span approximately one-quarter to one-seventh of an octave in the auditory nerve near threshold (see Table 1), which is the effective resolution of the input into the central auditory system. Measurements of frequency tuning width (referred to hereafter as bandwidth) at intermediate stages of the ascending auditory pathway in a variety of species showed preservation or enlargement of frequency bandwidth in single neurons. In anesthetized cats, frequency bandwidths have been measured in most stages of the ascending pathway. It has been shown that average frequency bandwidths increase from about 1/4th octave in the auditory nerve to about 1 octave in primary auditory cortex (A1) (Miller et al. 2002; Moshitch et al. 2006; Pickles 1979; Ramachandran et al. 1999). A similar trend was observed in a number of primate studies (see Table 1). One notable exception to this general trend of broadly tuned A1 neurons was the study by Recanzone et al. (2000) in awake macaque monkeys that showed sharp frequency tuning in a small number of sampled A1 neurons. A summary of previously reported bandwidths at various stages of the ascending auditory pathway in a variety of species is presented in Table 1. It is clear that in the vast majority of cases, A1 neurons were reported to have broad frequency tuning widths.

However, a recent study of the auditory cortex in awake human patients reported "ultrafine" frequency tuning (Bitterman et al. 2008). For the most sharply tuned neurons with best frequencies (BFs) ranging from a few hundred to ~2,000 Hz, estimated bandwidths were approximately one-twelfth of an octave, which is significantly narrower than that observed in auditory nerve of animals. Such narrow frequency tuning of auditory cortex neurons has not been observed previously in the auditory cortex of other mammals except in specialized species such as echolocating bats (Suga 1965). On the basis of this comparison, Bitterman et al. (2008) suggested that the human auditory cortex is specialized for fine frequency discrimination and that this fine frequency tuning might have arisen as a specialization for enhanced speech comprehension.

In the present study, we examined two major implications derived from the hypothesis that human auditory cortex is specialized for fine frequency tuning. First, we measured the frequency tuning width of auditory cortex neurons of another highly vocal primate species (the common marmoset, *Callithrix jacchus*) and compared them with those found in humans and other animals from previous studies. Because most of the previous studies of frequency tuning were conducted in anesthetized animals, a direct comparison between the neural responses of the auditory cortex of humans and nonhuman primates in the awake condition can shed light on whether there is indeed a specialization of human auditory cortex in frequency tuning. Second, we measured the frequency tuning properties of auditory thalamus neurons in awake marmosets to determine the extent to which the auditory cortex preserves, widens, or sharpens frequency tuning from its inputs.

On the basis of single-unit recordings in awake marmosets, we found that neurons in both the medial geniculate body (MGB) and A1 exhibited fine frequency tuning comparable to that observed in the Bitterman et al. (2008) study of human auditory cortex, suggesting that fine frequency tuning is not unique to human auditory cortex and is potentially generated at the level of the auditory thalamus or enhanced through a thalamus-cortex-thalamus loop.

MATERIALS AND METHODS

Animal preparation, acoustic stimuli, and single-unit recording procedures. All experiments conformed to protocols approved by the Johns Hopkins Institutional Animal Care and Use Committee

* E. L. Bartlett and S. Sadagopan contributed equally to this work.

Address for reprint requests and other correspondence: X. Wang, Dept. of Biomedical Engineering, Johns Hopkins Univ., 720 Rutland Ave., Traylor 410, Baltimore, MD 21205 (e-mail: xiaoqin.wang@jhu.edu).

Table 1. *Comparison of tuning widths reported in earlier studies of ascending auditory system and auditory cortex*

Study	Brain Region	Species/Anesthetics	Notes
Evans 1972	AN	Guinea pig/pentobarbital	Q_{10} range 1–4 ≤ 2 kHz, 3–10 > 2 kHz, only 1/100 units >10
Temchin et al. 2008	AN	Chinchilla/pentobarbital	Q_{10}, 6.0 ± 1.5 at 20 kHz, less for lower CF
Pickles 1979	AN	Cat/pentobarbital	Q_{10} = 5 at 1 kHz, 6 Hz at 3 kHz, 10 at 10 kHz
McLaughlin et al. 2008	AN	Cat/pentobarbital	Q_{10} = 5 at 1 kHz, 5.7 at 2 kHz
Harrison et al. 1981	AN	Guinea pig/awake/ketamine	All Q_{10} <12, only 2 units > 10 for tones <10 kHz
Harrison et al. 1981	AN	Human/awake	Compound action potentials. Q_{10}, 4.2 at 2 kHz, 6.5 at 4 kHz, and 8.5 at 8 kHz
Suga and Jen 1977	AN	Mustached bats/pentobarbital	Q_{10} mean = 83–84 at 61 kHz, mean = 9.0–9.3 at other freqs.
Davis et al. 2007	DNLL	Cat/decerebrate	All units Q_{10} <10, 54/62 units Q_{10} <8
Zhang and Kelly 2006	VNLL	Rat/ketamine/xylazine	Q_{10}, mean = 7.1, 9/70 > 10, mostly >10 kHz
Haplea et al. 1994	LL	Brown bat/Metofane/fentanyl	Q_{10}, 6/93 LL units > 20, most <10, 10–80 kHz
Egorova et al. 2001	IC	Mouse/ketamine/xylazine	Q_{10}, 17/114 units > 15, but only 2/17 had BFs <20 kHz
Aitkin et al. 1975	IC	Cat/pentobarbital	Q_{10}, 4/92 ICC units > 20, 8/92 > 10 all near 10–20 kHz
Ramachandran et al. 1999	IC	Cat/decerebrate	Q_{10}, all 134 units IC ≤ 10
Ryan and Miller 1978	IC	Awake monkey	Example units BW all > 0.25 octaves, no population data
Pollak and Bodenhamer 1981	IC	Mustached bat/awake	Q_{10}, mean = 122 at 61 kHz, mean = 18 at other freqs.
Haplea et al. 1994	IC	Brown bat/Metofane/fentanyl	Q_{10}, 26/122 IC units > 20, mostly 20–30 kHz
Miller et al. 2002	MGB/A1	Cat/ketamine	Avg MGB $Q_{1/e}$ = 5.8, <5% units > 12 MGB, Avg. A1 = 5.4
Edeline et al. 1999	MGB	Guinea pig/awake	Q_{10}, MGV max. <3, min. BW 500 Hz
Allon et al. 1981	MGB	Awake squirrel monkey	Q_{10} avg. 0.76 ± 0.85 <8 kHz, 3.42 ± 2.92 > 8 kHz
Suga et al. 1997	MGB	Mustached bat/awake	Q_{10} range 50–200 + for BF = 61 kHz
Llano and Feng 1999	MGB	Little brown bat/awake	Q_{10}, 7.2 ± 4.6 for 20–90 kHz tones
Sally and Kelly 1988	A1	Rat/Equithesin	Q_{10}, all BFs <10 kHz were <10, some >15 at high BF
Polley et al. 2007	A1, non-A1	Rat/pentobarbital	Q_{14}, all mean + SE values ≤ 3
Gaese and Ostwald 2001	A1	Rat/awake	Q_{10} 25–75% range, (19 units) 1.77–6.09
Linden et al. 2003	A1/AAF	Mouse/Domitor/ketamine	Q_{10} avg. 1.14 ± 0.10, A1, 0.86 ± 0.08, AAF
Bizley et al. 2005	A1, non-A1	Ferret/Domitor/ketamine	Q_{10} range 0–10
Moshitch et al. 2006	A1	Cat/halothane	Mean BW of large sample of units >1 octave
Qin et al. 2005	A1	Cat/awake	BW at half-max. rate, 0.45 ± 0.24 oct. for F0-sens. cells
Suga and Tsuzuki 1985	CF-CF area	Mustached bat/awake	Q_{10} 8–30 for 28–30 kHz, 50–300 for 61 kHz, 30–200 for 90 kHz
Philibert et al. 2005	A1	Marmoset/pentobarbital	Q_{10} range 2–7
Kajikawa et al. 2005	A1, CM	Marmoset/ketamine	Only 5/38 sites <.5 oct. BW 10 dB
Recanzone et al. 1993	A1	Owl monkey/Nembutal	Q_{10} average ≤3 untrained, 4–7 trained, Nearly all <10 Q_{10} behavior 25–42 for 3–8 kHz, approximately 100 for 2.5 kHz
Cheung et al. 2001	A1	Squirrel monkey/pentobarbital	Only 10/542 sites with Q_{10} > 10, BFs all <10 kHz
Pelleg-Toiba et al. 1989	A1	Squirrel monkey/awake	A1 mean BW_{10dB} = 0.4 oct.
Recanzone et al. 2000	A1, R, CM, L	Macaque/awake	A1 mean BW_{10dB} = 0.43, BW_{40dB} = 0.75. No early/late BW difference, mostly monotonic units.
Oxenham and Shera 2003	Psychophys.	Human/awake	Masking. Q_{10} approximately 10 at 1 kHz, 20 at 8 kHz
Bitterman et al. 2008	Auditory cortex	Human/awake	Q_{10} approximately 33 max. for units, 20 for average sharply tuned <2 kHz

AN, auditory nerve; LL, lateral lemniscus; DNLL, dorsal nucleus of LL; VNLL, ventral nucleus of LL; IC, inferior colliculus; MGB, medial geniculate body; MGV, ventral division of MGB; A1, primary auditory cortex; AAF, anterior auditory field; R, rostral division of auditory cortex; CM, caudomedial division of auditory cortex; L, lateral belt of auditory cortex; BW, bandwidth; BF, best frequency.

(IACUC). Details of experimental procedures for electrophysiological recordings from marmosets have been reported previously (Bartlett and Wang 2007; Lu et al. 2001). Briefly, marmosets were placed in a custom primate chair inside a double-walled soundproof booth (Industrial Acoustics). The interior of the booth was covered by 3-in. acoustic absorption foam (Sonex, Illbruck). The animals passively listened to the acoustic stimuli, with their behavioral state being monitored by the experimenter via a closed-circuit TV camera. The experimenter ensured that the animal's eyes were open prior to the delivery of each stimulus set. Recordings were performed with single high-impedance tungsten microelectrodes (2–4 MΩ), and unit isolation was established online with an 8-point template match and two additional adjustable amplitude-time windows when necessary (Alpha-Omega Engineering, Alpharetta, GA). Stimuli were generated digitally in MATLAB (MathWorks, Natick, MA) at a sampling rate of 97.7 kHz or 100 kHz with custom software, converted to analog signals (Tucker-Davies Technologies, Alachua, FL), power amplified (Crown Audio, Elkhart, IN), attenuated (Tucker-Davies Technologies), and presented from a loudspeaker (Fostex FT-28D, B&W-600S1 or B&W-600S3) situated ~70 cm (MGB recordings) or ~1 m (A1 recordings) in front of the animal. The loudspeaker had a flat frequency response curve (±5 dB) across the range of frequencies of the stimuli used, with a calibrated level (at 1 kHz) of ~90 dB SPL at a set level of 0 dB attenuation. We recorded from the right auditory cortex of two awake marmosets, the left auditory thalamus of two awake marmosets, and the right auditory thalamus of one awake marmoset. For A1 recordings, stimuli used were 100-ms-long pure tones with 5-ms cosine ramps, with frequencies that spanned 2–3 octaves around a manually determined center frequency in 0.1-octave steps (1/12th-octave steps were used in some cases). The range of sound levels covered was 0–80 dB in 20-dB steps. The best sound level (BL) of a neuron was defined as the sound level that elicited the maximal firing rate, determined by a near-BF tone over a 90-dB range in 5- or 10-dB steps. The BF of a neuron was defined as the centroid of the frequency tuning curve at BL. For MGB recordings, stimuli used were 200-ms-long pure tones with 5-ms linear ramps, with frequencies that spanned 2–4 octaves around a manually determined center frequency in 0.1-octave steps at a manually determined best level. With the tone frequency that evoked the maximum firing rate in the tuning curve, a rate-level curve was generated for sound levels from −10 to 80 dB in 10-dB steps. For many MGB neurons (n = 85), a second, denser frequency tuning curve (15–24 tones/oct.) was generated over a 1- to 2-octave range centered at the best frequency from the first tuning curve and at the best sound level determined from the

rate-level curve. For both A1 and MGB, responses to the complete stimulus set were acquired one repetition at a time. Within each repetition of the stimulus set, stimuli were presented in random order.

Analysis of A1 responses. Proximity to the lateral sulcus, strong tone responsiveness in the middle cortical layers, and clear tonotopy with at least one tonotopic reversal were the criteria used to determine the location of the neurons within A1. We recorded from well-isolated single neurons mostly located in the upper and middle cortical layers. We sampled uniformly across a wide range of frequencies (0.5–16 kHz) and sound levels (0–80 dB SPL). We found that many neurons in the MGB and A1 were difficult to drive if we did not sample densely enough or were inhibited if the sound level was too high.

Analysis methods used were similar to those described by Sadagopan and Wang (2008). We first verified that at least one stimulus evoked a significant excitatory response within a 150-ms window beginning 15 ms after stimulus onset, using the *t*-test ($P < 0.05$), compared with mean spontaneous activity over the entire stimulus set. Three hundred forty-eight of 460 sampled units met this criterion. Seventy-three units were excluded from additional analyses because either they responded only at the loudest level tested ($n = 34$) or their BF at one or more sound levels differed by more than two estimated bandwidths from the BF calculated at the BL ($n = 39$).

Frequency tuning curves (i.e., firing rate vs. tone frequency) of the remaining 275 units were then computed at each level and thresholded at 20% of peak response. Threshold for a unit was therefore defined as the lowest sound intensity at which the evoked response was at least 20% of the maximum response. Tuning curves were interpolated and smoothed, using a five-point moving window for display. We then fit an area-matched rectangle to a tuning curve at a given sound level by fixing its position at the centroid of the tuning curve and its height at maximum firing rate. The calculated widths of the rectangles were then taken as measures of bandwidth at that sound level. The rectangle fit method closely approximates the half-maximal width for perfectly Gaussian tuning curves and takes into account long-tailed tuning curves, giving an upper bound for bandwidth estimates. The bandwidth of the unit was taken as the bandwidth at BL. These values were computed over the entire response duration and over the last 100 ms of the response window (sustained) in order to observe whether frequency tuning changes over the course of the response. To compute population tuning curves, individual tuning curves were normalized by the maximum driven rate (after subtraction of spontaneous rate) and centered at the unit's BF. We then interpolated each individual tuning curve in 0.1-octave steps to ±1 octave to ensure uniformity across the population and then averaged all tuning curves at the BL or at 10 dB above threshold for each unit. The full width at half-maximum (FWHM) of the population tuning curve was taken to be its bandwidth. For comparison with previous studies, Q values for each unit were calculated by dividing the BF of each unit (in kHz) by its bandwidth (in kHz) at the BL or at 10 dB above threshold. In cases where a 20-dB sampling resolution was used, the bandwidth at 10 dB above threshold was obtained by linearly interpolating between the bandwidths at threshold and 20 dB above threshold.

Analysis of MGB responses. The responses of 191 MGB units were recorded from three marmosets in response to 200-ms tone stimuli. A unit was considered to have a defined BF if it had a significant excitatory response ($P < 0.05$, Wilcoxon rank sum vs. spontaneous activity) and the firing rate of the unit dropped to <50% of the maximum firing rate on at least one side of the BF in the tuning curve. One hundred fifty-nine of 191 units met these criteria, with BFs ranging from 0.6 to 32.5 kHz. Among 159 units, 73 units were located in the ventral division (MGV). The remaining 86 units were localized in non-MGV subdivisions (72 units) or were too close to borders between MGB subdivisions to classify their location (14 units).

Bandwidth for an MGB neuron was determined as the tuning width (expressed in octaves or kilohertz) at which the tuning curve fell below 50% of the firing rate maximum at BF. The 50% tuning width boundary was determined by linearly interpolating between adjacent MGB responses that were above and below 50%. Population tuning curves and Q value at BL (Q_{BL}) were computed in the same way as for A1 units.

MGB anatomy. To confirm recording locations, electrolytic lesions were made in physiologically identified regions of MGB by passing 2- to 10-μA current through the recording electrode (6–10 s each polarity). MGB subdivisions were assigned based on parcellation schemes established in previous studies of the MGB in macaques (Molinari et al. 1995) and marmosets (Aitkin et al. 1988; de la Mothe et al. 2006). The locations of recorded neurons in the MGB were reconstructed based on the coordinates of the electrode tracks relative to the tracks in which lesions were made and the depths at which the recordings occurred.

RESULTS

Distributions of tuning bandwidths in A1 and MGB. Data presented in this study are based on 275 tone-responsive single units from A1 and 159 tone-responsive single units from all subdivisions of the auditory thalamus (MGB). These units had significant excitatory responses to at least one pure tone in our stimulus set and a well-defined BF (see MATERIALS AND METHODS). Bandwidths of all neurons were calculated as described above, and the distributions of bandwidths for A1 and MGB neurons are plotted in Fig. 1*A*. Cumulative distributions of A1 and MGB bandwidths are plotted in Fig. 1*B*. The key observation from these data is that many A1 units (27%) and a large fraction of MGB units (76%) show frequency tuning bandwidths that are less than the frequency tuning bandwidths typically observed in auditory nerve fibers—which, in a variety

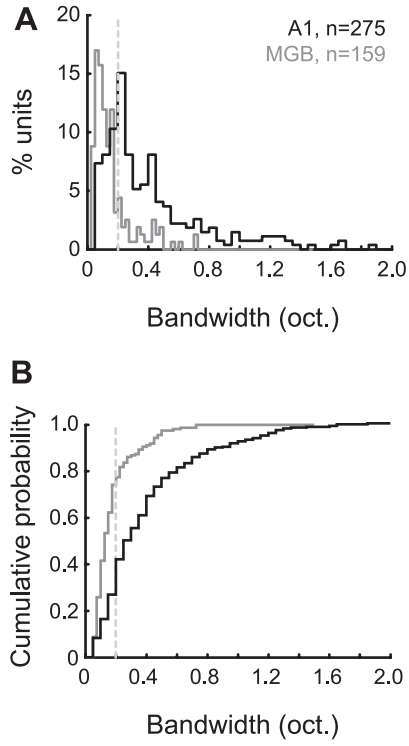

Fig. 1. Primary auditory cortex (A1) and medial geniculate body (MGB) tuning bandwidths. *A*: distributions of bandwidths [at best sound level (BL)] for all A1 units ($n = 275$, black) and MGB units ($n = 159$, gray). *B*: cumulative distributions of A1 (black) and MGB (gray) bandwidths. Light gray dashed line indicates the typical bandwidth of auditory nerve fibers (0.2 oct.) that was used as a boundary to classify sharply tuned units from the rest of the population.

of species, has been reported to be ~0.2 octaves (Evans 1972; Pickles 1979; Temchin et al. 2008; see Table 1). Such high numbers of finely tuned neurons in both cortex and thalamus have seldom been reported in earlier studies (see Table 1). These sharply tuned neurons have tuning bandwidths that are similar to that reported by a study in human auditory cortex (Bitterman et al. 2008), and are therefore of special interest. But this population also raises several questions: For example, are sharply tuned neurons a functionally specialized population? Are they restricted to any behaviorally relevant frequency range? Do they show different response dynamics? To study these properties in detail, and to investigate whether these neurons show any differences from the rest of the population, we divided the A1 and MGB populations into "sharply tuned" (ST) and "not sharply tuned" (NST) categories. For both A1 and MGB, we chose the typical auditory nerve bandwidth of 0.2 octaves as the boundary between these two classes (gray dashed line in Fig. 1). Note that the cutoff bandwidth used to categorize responses as ST or NST does not imply a priori that there are distinct neuron classes or that there is an underlying bimodal distribution of bandwidths among A1 or MGB neurons. Rather, this boundary is chosen merely to develop a better characterization of the ST neurons that are a behaviorally interesting subset. In the next sections, we analyze and compare the properties of ST and NST neurons in A1 and MGB in detail.

Auditory cortex frequency tuning properties. A1 neurons were divided into two groups: those with frequency bandwidth <0.2 octaves were referred to as "sharply tuned" (ST group: 74/275, 27%), and the rest of the population were referred to as "not sharply tuned" (NST group: 201/275, 73%). The proportion of neurons classified as ST or NST did not depend on the bandwidth metric used. Similar results were obtained by both using the rectangle fits (27% ST, mean ST bandwidth = 0.125 oct.) and calculating bandwidth at half-maximal rate without accounting for long-tailed tuning curves (32% ST, mean ST bandwidth = 0.115 oct.), with no significant changes in the physiological properties of the ST or NST population. Therefore, all values for A1 neurons reported in this article were derived with the more conservative rectangle-fit procedure (see MATERIALS AND METHODS). We did not find any systematic dependencies of tuning widths on BF. However, two important differences were evident between ST and NST groups: *1*) spontaneous firing rates of the ST group were significantly less than those of the NST group and *2*) maximum driven rates of the ST group were significantly less than those of the NST group (Table 2).

Figure 2, *A* and *B*, shows the dot raster and frequency response area (FRA) of a typical ST neuron. In this example, significant responses to 50-ms pure tones were restricted to a single frequency bin (bin size = 1/10th oct.) and two sound level bins (bin size = 20 dB). The FRA of this neuron shows typical "O"-shaped tuning to both frequency and intensity with a well-defined BF and BL (Sadagopan and Wang 2008). We calculated the frequency bandwidths for the population of 275 A1 neurons (see Table 2). It should be emphasized that we measured the frequency bandwidth at the BL for all neurons, where response rate was strongest. Note that a large fraction of neurons in A1 of awake marmosets are tuned to sound level, with a median level-tuning width of 25 dB (Sadagopan and Wang 2008). Expressed in terms of a quality factor or Q value, these bandwidths translate to Q_{BL} of 12.1 ± 4.8 for ST units and 3.7 ± 1.8 for NST units (Table 2). For comparison with previous data, we also evaluated Q values at a sound level 10 dB above threshold. In this case, Q_{10} values were 14.3 ± 3.9 for ST units and 6.6 ± 4.8 for NST units (Table 2). These data show that, on average, the bandwidth at 10 dB above threshold is smaller than the bandwidth at BL. Furthermore, for level-tuned units, bandwidth decreased at louder levels as well (Sadagopan and Wang 2008). Therefore, bandwidth at BL typically corresponds to the broadest point in a given neuron's tuning curve and is a conservative estimate of a neuron's bandwidth.

In Fig. 2*C*, we computed the normalized population average frequency tuning curves for the entire A1 population of 275 units at BL. The population average frequency tuning curves were centered at BF and extended up to 1 octave above and below BF. Averages were computed for the entire response duration [ON+SUS, analysis window: (stimulus onset + 15 ms, stimulus offset + 50 ms)] and for the sustained response alone [SUS, analysis window: (stimulus onset + 50 ms, stimulus offset + 50 ms)]. For the entire response duration, the bandwidth measured from the population average frequency tuning curve was 0.5 octaves. For the sustained portion of the response, the mean bandwidth was even narrower, 0.38 octaves (Fig. 2*C*). When we repeated the same analyses for units in the ST group, the mean bandwidth was 0.125 octaves for the entire response duration, which reduced to <0.1 octaves (minimum sampling resolution) during the sustained portion of the response (Fig. 2*D*). It should also be

Table 2. *Response properties of units with ST and NST groups in auditory thalamus and cortex*

	A1-ST (74/275, 27%)	A1-NST (201/275, 73%)	MGV-ST (59/73, 81%)	MGV-NST (14/73, 19%)	Non-MGV-ST (62/86, 72%)	Non-MGV-NST (24/86, 28%)
Spont. Rate, sp/s	2.7 ± 6.4[b]	7.5 ± 9.6	9.3 ± 7.3	9.4 ± 6.8	9.3 ± 5.8	8.1 ± 7.1
Max. Rate, sp/s	30.3 ± 27.8[b]	48.8 ± 42.5	31.4 ± 21.2	34.4 ± 37.3	24.8 ± 14.1	26.4 ± 22.6
Bandwidth, oct.	0.125 ± 0.041[a]	0.54 ± 0.37[d]	0.11 ± 0.04	0.34 ± 0.15	0.12 ± 0.04	0.39 ± 0.14
Bandwidth, Hz	716 ± 507	2,593 ± 2,888	680 ± 480	1,021 ± 696	644 ± 690	1,464 ± 1,509
Q_{BL}	12.1 ± 4.8[c]	3.7 ± 1.8	15.9 ± 6.2	4.9 ± 1.8	14.2 ± 5.8	4.3 ± 1.5
Best frequency, kHz	7.7 ± 4.5	7.0 ± 5.0	9.7 ± 5.6[e]	5.5 ± 4.5	7.8 ± 6.6	6.3 ± 7.0

All reported values are means ± SD. ST, sharply tuned; NST, not sharply tuned; Q_{BL}, Q value at best sound level. Maximum response rate (Max. Rate) was computed over the entire stimulus duration [spontaneous rate (Spont. Rate) has been subtracted]. [a]A1-ST mean bandwidth sharpens to <0.1 octave during the sustained response, comparable to MGB-ST units. [b]Significantly different from A1-NST, $P < 0.001$, Wilcoxon rank sum test. [c]A1-ST and A1-NST Q_{10} values are 14.3 ± 3.9 and 6.6 ± 4.8, respectively. [d]A1-NST mean bandwidth sharpens to 0.35 octave during the sustained response. [e]Significantly different from non-MGV-ST, $P < 0.02$, Wilcoxon rank sum test.

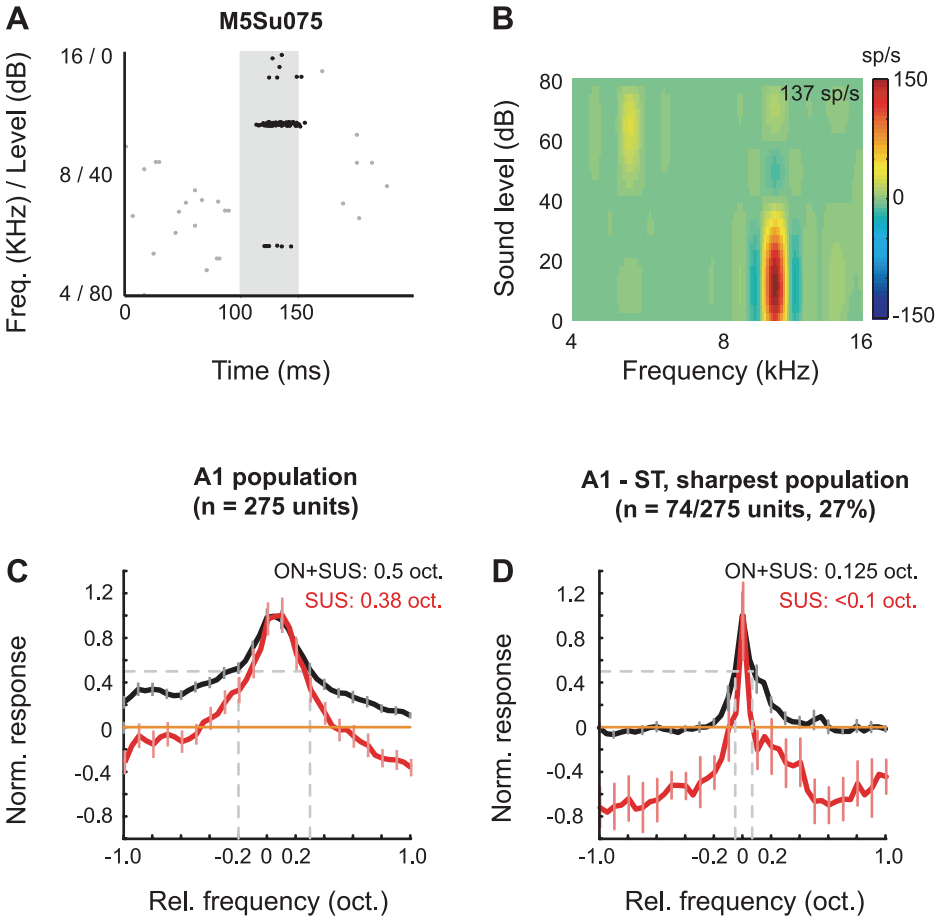

Fig. 2. A1 single-neuron and population tuning properties. *A* and *B*: example spike raster and frequency response area of an A1 neuron. Shaded area in *A* is stimulus duration (50-ms pure tones in this case; both frequency and level were varied), black dots are spikes falling within analysis window, and gray dots are spontaneous spikes. Frequency and sound level are interleaved on the *y*-axis. This neuron was tuned to a single frequency bin (0.1-oct. sampling resolution) and also tuned to sound level (*B*). *C*: population tuning curves for entire population of A1 neurons computed during entire response duration (ON+SUS, black lines) and during sustained response alone (SUS, red lines). Orange line indicates baseline; gray lines delineate frequency tuning bandwidth at 50% maximal response for the entire response duration. Sharpening of the tuning curve is evident during the sustained portion of the response. *D*: same as in *C*, but computed for the sharpest 27% of A1 neurons (ST units). For this population, mean tuning width was 0.125 octaves over the entire response duration and <0.1 octaves during the sustained portion of the response. Significant lateral suppression also developed over response duration (red line). All plots are means ± SE.

noted that there was significant lateral off-BF suppression (depression of population response rate below spontaneous rate; Sadagopan and Wang 2010) during the sustained response in the A1 responses, especially in the ST units (see red lines in Fig. 2, *C* and *D*).

Auditory thalamus frequency tuning properties. Of the 191 MGB units recorded from three marmosets, 159 had significant excitatory responses and well-defined BFs (see MATERIALS AND METHODS), including 73 MGV units. They had BFs ranging from 0.6 to 32.5 kHz. With the same criterion as A1 units, MGB units were classified as "sharply tuned" (ST) if their bandwidths were ≤0.2 octaves. The rest of the units were classified as "not sharply tuned" (NST). In the MGB, ST units constituted a majority of units in the auditory core MGV subdivision (81%, 59/73 units; see Table 2), and they constituted a majority of neurons in the remainder of the MGB (72%, 62/86 units). The spontaneous firing rates and driven rates of ST and NST MGB units were not significantly different (Table 2), in contrast to their counterparts in A1.

One example of an MGB ST unit is shown in Fig. 3, *A* and *B*. For this unit, the frequency tuning curve was measured at BL with pure tones at a high sampling density (24 tones/oct.). Only tones at 9.4 and 9.71 kHz produced significantly driven responses, and these responses were sustained for the tone duration (Fig. 3, *A* and *B*). The half-width of this unit was 0.083 octaves (1/12th oct.). Significant suppression was evident, particularly on the low-frequency side of the tuning curve at 8.6 kHz (Fig. 3, *A* and *B*). Figure 3*C* shows another unit in which significant suppression was present on the low-frequency side and high-frequency side of the tuning peak. In this example, the suppression occurred at frequencies close to BF (0.05 oct. away on the low-frequency side, 0.1 oct. away on the high-frequency side) and was sharply tuned.

The distribution of bandwidths at BL in the MGB is plotted in Fig. 3*D*. For MGB neurons, the 25–75% range of BLs was 20–60 dB SPL, with a median of 40 dB. Most MGV units (Fig. 3*D*, black bars) were ST units (<0.2 oct., left of dashed line). Surprisingly, we found that many units from non-MGV subdivisions (Fig. 3*D*, gray bars) were also sharply tuned. There did not appear to be two distinct populations for frequency tuning. Instead, the distribution of bandwidths peaked on the bin centered at 0.1-octave bandwidth, and then the number of units decreased as tuning bandwidth increased. Bandwidths >0.2 octaves were dominated by units from non-MGV subdivisions. For a subset of 25 MGB units whose BL was 10 dB above threshold, the tuning bandwidths (0.13 ± 0.10 oct.), Q_{10} values (14.4 ± 7.5), and proportion of ST units (22/25 = 88%) were not significantly different from the values measured for the population at BL.

In Fig. 3*E*, the frequency tuning curves of all MGB units were normalized relative to the response at BF and averaged. Black and gray lines indicate the normalized tuning curve over the entire response duration and the sustained response portion (100–200 ms after stimulus onset), respectively. The two population average tuning curves were quite similar. The mean bandwidth of all MGB units was ~0.14 octaves (Table 2). Such small bandwidths for the population reflect that most MGB neurons were ST units (76%). In Fig. 3*F*, the frequency

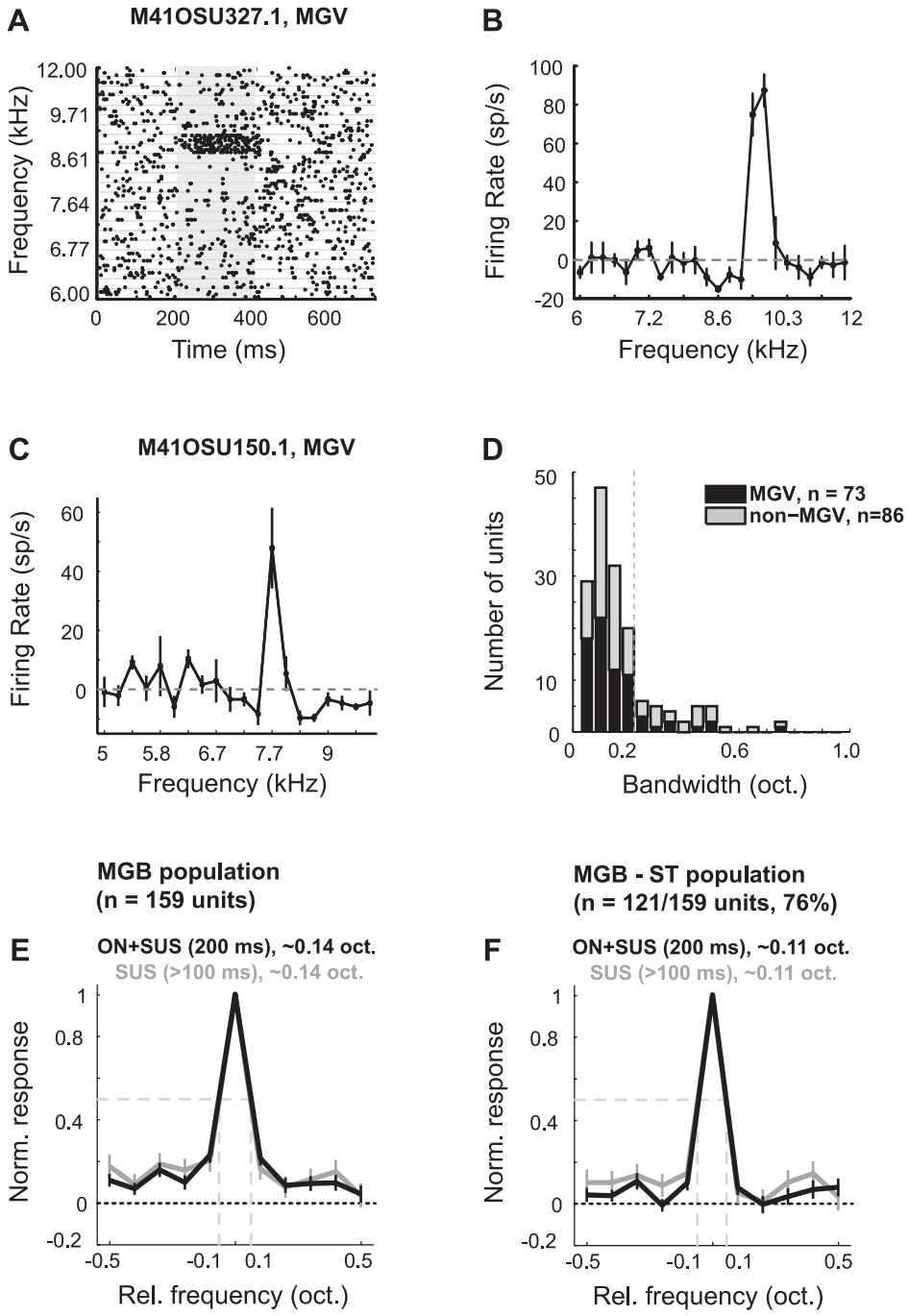

Fig. 3. Auditory thalamus single-neuron and population tuning properties. *A* and *B*: example spike raster and frequency tuning curve of a MGB ventral division (MGV) neuron (unit M41OSU327.1). Sound level = 30 dB SPL. Shaded area in *A* is stimulus duration (200-ms pure tones). Black dots are spikes. Clear responses occur only in 2 frequency bins (1/24th oct. spacing), also apparent in the frequency tuning curve in *B*. *C*: example frequency tuning curve of an MGV neuron with clear suppression on the low- and high-frequency sides of the tuning curve peak (unit M41OSU150.1). Sound level = 10 dB SPL. *D*: distribution of frequency tuning bandwidth at best level for MGB neurons, separated into neurons from MGV (black bars) and MGB neurons from non-MGV subdivisions (gray bars). Gray dashed line at 0.2-octave bandwidth separates units classified as sharply tuned (ST) or not sharply tuned (NST). *E*: population tuning curves for MGB neurons. Population tuning curves were computed over the entire response duration (ON+SUS, black line) or only during the sustained portion of the response, 100–200 ms after stimulus onset (SUS, gray line). Black dotted line indicates baseline. Light gray dashed lines delineate the frequency tuning bandwidth at 50% maximal response for the entire response duration. *F*: same as in *E*, but computed for ST units whose tuning bandwidths were <0.2 octaves. All plots are means ± SE.

tuning curves of MGB ST units were normalized relative to the response at BF and averaged. The two population average tuning curves for the entire stimulus duration (black line) and the sustained portion (gray line) were quite similar. The mean bandwidth of MGB ST units was 0.11 octaves (Table 2), with some bandwidths as small as 0.05 octaves, but there was no significant difference between the bandwidths of the total and sustained responses (Fig. 3*F*). Suppression at off-BF frequencies was common in the ST population, with 55 of 121 ST units having firing rates below spontaneous rates at −0.1 octaves away from BF and 56 of 121 ST units at +0.1 octaves away from BF. By definition, MGB NST units had significantly larger bandwidths (Table 2). There was again no significant difference between the bandwidths of the total and sustained responses of the MGB NST units. The lack of difference in bandwidth between the total and sustained responses in MGB is in contrast to what was observed in A1 (Fig. 2, *C* and *D*).

Dependence of frequency tuning measures on BF. We examined more closely the relationship between BF and measures of frequency tuning sharpness, using a variety of measures to enable comparison with other studies. In A1, we found no significant differences in the BF distributions of ST and NST units (Fig. 4*A*; $P = 0.43$, Kolmogorov-Smirnoff test). The greatest proportion of ST units was encountered in the BF range of 4–8 kHz. Bandwidth (in kHz) increases approximately linearly with increasing BF for both ST and NST units

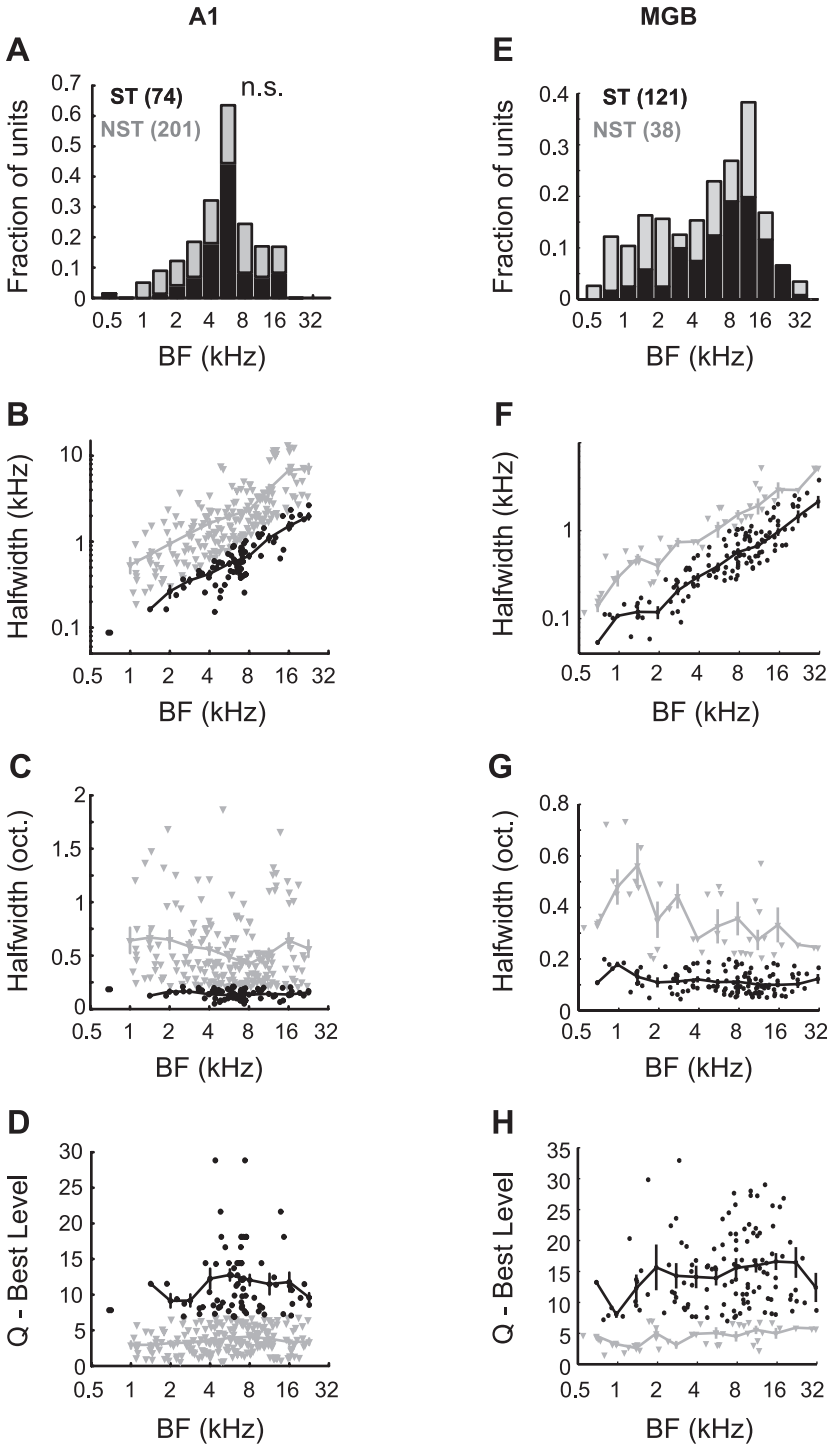

Fig. 4. A1 and MGB frequency tuning as a function of best frequency (BF). *A*: normalized BF distributions for ST (black bars) and NST (gray bars) units in A1. Bin width = 1/2 octave. The distributions were not statistically significant (n.s.; $P = 0.43$, Kolmogorov-Smirnoff test). *B*: bandwidth in kilohertz at half-maximal rate as a function of BF. In *B–D*, black circles represent ST units and gray triangles NST units. The mean and SE are plotted in 1/2-octave intervals. *C*: bandwidth in octaves as a function of BF. Same format as *B*. *D*: Q value at BL (Q_{BL}) as a function of BF. Same format as *B*. *E*: normalized BF distributions for ST (black bars) and NST (gray bars) units in MGB. Bin width = 1/2 octave. The distributions were significantly different ($P < 0.01$, Kolmogorov-Smirnoff test). *F–H*: bandwidth measures as a function of BF for MGB units. Same format as *B–D*.

and with similar slopes (Fig. 4*B*). When we plotted bandwidth (in oct.) and Q_{BL} as a function of BF, no observable differences were evident between the ST and NST units (Fig. 4, *C* and *D*), indicating that ST and NST units were similarly tuned across the frequency range and reinforcing the observation that ST units were prevalent across the entire frequency range.

In the MGB, BFs of ST units were significantly higher than those of NST units (Fig. 4*E*; $P < 0.002$, Kolmogorov-Smirnoff test). MGB neurons were sampled throughout its extent, including MGV neurons that are part of the core auditory pathway and posterodorsal MGB neurons that are part of the belt pathway (de la Mothe et al. 2006), but not including neurons from the medial division of MGB or the suprageniculate nucleus. Across the MGB population, the units in the bottom quartile of the BF distribution (<2.9 kHz, $n = 40$) differed from the other units ($n = 119$) in that they exhibited broader bandwidths (0.26 ± 0.19 oct. compared with 0.14 ± 0.10 oct. for units with BFs >2.9 kHz; $P < 0.003$, Kolmogorov-Smirnoff test) and a lower proportion of ST units (55% vs. 83% for units with BFs >2.9 kHz; $P < 0.001$ χ^2-test). Figure 4*E* shows the distribution of BFs for proportion of ST (black bars) and NST units (gray bars) where the distribution of BF

has been separated into 1/2-octave bins. The bandwidths (in kHz) of ST and NST units increased approximately linearly with increasing BF with similar slopes (Fig. 4*F*). As BF increased, the bandwidths (in oct.) of ST units did not change, but the bandwidths of NST units decreased as BF increased up to ~4 kHz and stayed unchanged at higher BFs (Fig. 4*G*). Similarly, Q_{BL} of ST units did not change as a function of BF, but they did increase slowly with BF (to ~4 kHz) for NST units (Fig. 4*H*).

DISCUSSION

By comparing frequency tuning properties between the marmoset MGB and A1, we drew the following conclusions. *1*) A large population of neurons in both the MGB (76% overall) and A1 (27%) were sharply tuned, to the order of 1/7th to 1/20th of an octave (Table 2), significantly sharper than earlier reported animal data (Table 1) and comparable to recently reported human data (Bitterman et al. 2008). This suggests that fine frequency tuning may not be a unique feature of human auditory cortex. *2*) Sharpness of tuning in A1 may not be a de novo cortical property, as many MGB neurons exhibited as sharp or sharper tuning than cortical neurons. *3*) Sharpening of frequency tuning during the sustained response after the stimulus onset response was observed in A1 (Fig. 2, *C* and *D*) but not MGB (Fig. 3, *E* and *F*), suggesting that thalamocortical or intracortical dynamics restore the frequency selectivity of their MGB inputs after a less selective onset response. *4*) Sharp frequency tuning was observed across the entire range of observed BFs in both A1 and MGB recordings (Fig. 4, *A* and *E*), although ST units were less common in units whose BFs were <3 kHz.

Until recently, sharp frequency tuning had not been clearly demonstrated in the auditory cortex and auditory thalamus of species other than bats (Suga 1965; Suga and Jen 1977; Suga et al. 1997). Data from a variety of species and recording preparations indicated that frequency tuning measurements in the auditory thalamus and auditory cortex were at least as broadly tuned as the auditory nerve (Calford 1983; Doron et al. 2002; Edeline et al. 1999; Kajikawa et al. 2005; Qin et al. 2005; Rauschecker et al. 1997). Table 1 summarizes results from a number of studies at different levels of the auditory pathway and in different species. Auditory nerve tuning is fairly similar across species, with Q_{10} values ranging from 3 to 10 (Table 1). This includes auditory nerve tuning in mustached bats at frequencies away from the hyperacute 61-kHz region, while the fibers tuned near 61 kHz have exceptionally sharp tuning (Q_{10} mean >80, Suga and Jen 1977). Rhode et al. (2010) concluded that frequency tuning in marmoset and squirrel monkey cochlear nucleus neurons was similar to the auditory nerve tuning found in other species. Earlier studies showed that frequency tuning inferior colliculus (IC) units was comparable to that observed in the auditory nerve in awake monkeys (Ryan and Miller 1978) or in cats (McLaughlin et al. 2008; Ramachandran et al. 1999), but there may be slight sharpening in the IC of bats (Haplea et al. 1994; Pollak and Bodenhamer 1981). Therefore, although we do not have data on the tuning of marmoset IC neurons, the data from the cochlear nuclei of marmosets and the IC of other species suggest that the fine frequency tuning observed in MGB and A1 may originate in MGB.

The changes in frequency tuning width from auditory nerve to A1 differs widely between reported studies, although nearly all studies in cats and rodents exhibit broader tuning in A1 responses, regardless of anesthetic state (Table 1). Studies in anesthetized marmoset and other monkeys have demonstrated Q_{10} values <7 (Table 1, Philibert et al. 2005), which is comparable to auditory nerve responses in other studies. In one study, A1 units in owl monkeys trained in an auditory discrimination task were found to exhibit higher Q_{10} values near the training frequencies compared with untrained owl monkeys (Recanzone et al. 1993). Auditory cortex neurons in mustached bats exhibit exquisite tuning in the 61-kHz region that is even sharper than auditory nerve responses, with Q_{10} values reaching 200–300, but with little or no sharpening at other frequencies (Suga and Tsuzuki 1985). Other than bats, the only evidence of fine frequency tuning in A1 (defined in this study to be tuning width narrower than typical auditory nerve tuning, ~0.2 oct.) was provided in a study by Recanzone et al. (2000) in awake macaque monkeys, where a small number of A1 neurons had bandwidths (at 10 dB above threshold) smaller than 0.2 octaves (see Fig. 12A of Recanzone et al. 2000). The mean bandwidth of the A1 population was 0.43 octaves at 10 dB above threshold as reported by Recanzone et al. (2000).

Fewer A1 neurons were classified as "sharply tuned" (27%) compared with MGB neurons (76%) in the present study. Broader bandwidths in the population of A1 neurons (ST and NST combined) could arise from narrower feed-forward MGB inputs because of two possibilities that require further investigation: *1*) A1 neurons might integrate inputs from sharply tuned MGB neurons that have nearby BFs or *2*) A1 neurons may receive inputs from MGB neurons at the same BF but having different bandwidths. In our population of A1 neurons, a sharpening of frequency tuning developed over response duration that was not observed in MGB neurons, causing the frequency resolution of the A1 population to approach that of the MGB population. This sharpening could result from several mechanisms that need further investigation. First, late intracortical inhibition could suppress responses to off-BF frequencies. Second, the onset response in A1 might reflect convergence of many MGB inputs, whereas the sustained response might be representative of fewer thalamic inputs. Third, excitatory drive to cortical neurons might be reduced during the sustained response due to synaptic depression or spike rate adaptation at lower processing stages, resulting in an "iceberg effect" that could lead to sharper tuning. Finally, feedback projections from A1 to MGB might also sharpen frequency tuning. Therefore, the relationship between A1 and MGB with respect to frequency selectivity can be summarized as follows. When measured over the entire response duration, fewer A1 neurons are sharply tuned compared with MGB neurons, and MGB-ST neurons show slightly higher selectivity compared with A1-ST neurons (Table 2). However, because of the differential sharpening of A1 tuning over response duration, some A1-ST neurons become more selective than MGB-ST neurons during the sustained response. Note that it is also likely that the fraction of sharply tuned A1 neurons increases during the sustained response. The various mechanisms that are active in shaping tuning curves is a question left open for future experiments.

The frequency tuning bandwidths reported in this study were measured at each unit's BL (unless specified), which ranged

widely from unit to unit. The difference between BL and threshold was 16 ± 18 dB for MGB units (n = 111) and 19.4 ± 22 dB for A1 units (n = 275). Frequency tuning of most A1 neurons in awake marmosets does not widen substantially with increasing sound level (Sadagopan and Wang 2008) but does exhibit some widening within the range of sound levels a given neuron typically responds to (median 25 dB level tuning width). For the well-defined FRAs of the cortical neurons analyzed in this study, it is unlikely that the 20-dB intensity steps would substantially affect the interpolated Q_{10} values, even if level tuning is I-shaped or O-shaped because the width of the level tuning is >20 dB for A1 units in awake marmosets (see Fig. 4D of Sadagopan and Wang 2008). If the true BL were 20 dB above threshold, then at worst the Q_{10} value would be as wide as the Q_{BL}. These values (Q_{10} = 14.3, Q_{BL} = 12.1) are slightly different but do not detract from the main point that there is a substantial population of A1 neurons whose bandwidths are much sharper than auditory nerve bandwidths. If the true BL were only 10 dB above threshold, such that $Q_{10} = Q_{BL}$, then it is possible that the Q values at 20 dB could be overestimated. However, the subset of MGB neurons whose BL was 10 dB above thresholds had Q values that were similar to the rest of the MGB population. We also reported earlier that Q_{10} was sharper than Q_{BL} for a large population of A1 units (Sadagopan and Wang 2008). For "V" units that were tuned monotonically to sound level (loudest sound level was taken as BL for these units), bandwidth usually increased with increasing sound level and was at its maximum at BL for most neurons. Therefore, bandwidths of the cortical population presented in this study are estimates at the broadest point of the neurons' tuning curves. Despite this important difference, data from our study are comparable to tuning bandwidths reported for single units in human A1 (Bitterman et al. 2008). In the study by Bitterman et al. (2008), sounds were presented at moderate levels that were comfortable for the subjects, but were not referenced to each neuron's preferred sound level. Another stimulus parameter that affects bandwidth measurement is stimulus density. For example, it has been reported that excitatory tuning width decreases and inhibitory tuning width increases with increasing spectral density (Blake and Merzenich 2002). This is attributable to the presence of energy within the lateral suppressive or inhibitory sidebands of cortical neurons (Wu et al. 2008). In the present study, we presented pure tones one at a time, in contrast to simultaneously presented multiple tones ("chord" stimuli) in the study by Bitterman et al. (2008). It is quite likely that we would have observed even smaller bandwidths had we used stimuli of higher density such as random spectral stimuli (Barbour and Wang 2003) or random chord stimuli (Bitterman et al. 2008; Blake and Merzenich 2002).

An important factor that may further affect these results is the anesthetic state of the animal, which modulates the underlying balance of excitatory and inhibitory inputs to a neuron, and therefore its tuning bandwidth. For example, changes to bandwidth as a function of anesthesia have been documented in rats (Gaese and Ostwald 2001). For marmosets, the bandwidths of auditory thalamus and cortex units (Figs. 2 and 3) are significantly narrower in the awake condition (the present study) than in ketamine- or pentobarbital-anesthetized conditions (Philibert et al. 2005). Similarly, in awake macaque monkeys, Recanzone et al. (2000) observed finely tuned A1 neurons with bandwidths smaller than or similar to that of the auditory nerve. It should be noted that fine frequency tuning reported in humans was measured when the subjects were awake and alert (Bitterman et al. 2008). Collectively, this evidence suggests that sharper frequency tuning in auditory cortex would be observed if measured in the awake state.

The effect of attention, or other behaviors, on the frequency tuning of individual A1 neurons is largely unclear. In owl monkeys trained on a frequency discrimination task, Recanzone et al. (1993) showed that, in addition to an increase in cortical area at the trained frequency, neurons were also more sharply tuned within this frequency range compared with passively listening monkeys. Alternatively, another neural mechanism that can underlie improved behavioral frequency discrimination is the enhancement of spectral contrast by suppression of responses at the target frequency and enhancement at nearby frequencies, typically observed when aversive conditioning stimuli are used (Ohl and Scheich 1996). In sharp contrast, Brown et al. (2004) reported that frequency discrimination training in cats did not affect the topography of primary auditory cortex, although the cats showed improved discrimination at the target frequencies. Rather than a sharpening of tuning curve at BF, the Brown et al. (2004) study showed that tuning curves became broader at frequencies slightly higher than the target frequency. Therefore, depending on the type of task (detection vs. discrimination) and the type of reinforcement (positive vs. aversive), A1 neurons may sharpen, broaden, or suppress responses at target frequencies. While the frequency tuning of A1 neurons appears to be amenable to top-down plasticity effects and behavioral modulation, only certain types of manipulations may result in further sharpening of A1 tuning curves.

Our results demonstrate that human auditory cortex is not alone in exhibiting sharp frequency tuning, and that sharp frequency tuning may not be of cortical origin. It remains to be seen whether the fine frequency tuning is limited to primate species or can also be found in other mammalian species besides bats. The lower spontaneous rates and lower driven rates of ST units may indicate that they are under a stronger tonic inhibitory influence. The existence of finely tuned neurons does not imply that a fine-grained place-coding of frequency by such neurons directly underlies behavioral frequency discrimination. Many population-coding schema may be derived to explain the development of apparent hyperacuity at the level of auditory cortex. However, these finely tuned neurons could only serve to sharpen frequency discrimination regardless of read-out mechanisms. For example, because of their sharp tuning aided by lateral suppression, these neurons also show steeper tuning curve slopes that may be used in a slope-based coding scheme to provide finer frequency difference estimates. In conclusion, we have demonstrated that neurons in both A1 and MGB of awake marmosets show fine frequency tuning comparable to that observed by Bitterman et al. (2008) in alert humans. Although several experimental differences exist, we have provided a strong counter-example to the hypothesis that fine frequency tuning is a specialized property of human auditory cortex neurons.

ACKNOWLEDGMENTS

We thank Dr. Stewart Hendry and Ashley Pistorio for help with neuroanatomy and Ashley Pistorio and Jenny Estes for assistance in animal care and surgical assistance.

Present addresses: E. L. Bartlett, Depts. of Biological Sciences and Biomedical Engineering, Purdue University, West Lafayette, IN 47907; S. Sadagopan, Laboratory of Neural Systems, Rockefeller University, New York, NY 10065.

GRANTS

This work was supported by the Deafness Research Foundation (E. L. Bartlett) and National Institute on Deafness and Other Communication Disorders Grants DC-006357 (E. L. Bartlett) and DC-003180 and DC-005808 (X. Wang).

DISCLOSURES

No conflicts of interest, financial or otherwise, are declared by the author(s).

REFERENCES

Aitkin LM, Webster WR, Veale JL, Crosby DC. Inferior colliculus. I. Comparison of response properties of neurons in central, pericentral, and external nuclei of adult cat. *J Neurophysiol* 38: 1196–1207, 1975.

Aitkin LM, Kudo M, Irvine DR. Connections of the primary auditory cortex in the common marmoset, *Callithrix jacchus jacchus*. *J Comp Neurol* 269: 235–248, 1988.

Allon N, Yeshurun Y, Wollberg Z. Responses of single cells in the medial geniculate body of awake squirrel monkeys. *Exp Brain Res* 41: 222–232, 1981.

Barbour DL, Wang X. Contrast tuning in auditory cortex. *Science* 299: 1073–1075, 2003.

Bartlett EL, Wang X. Neural representations of temporally modulated signals in the auditory thalamus of awake primates. *J Neurophysiol* 97: 1005–1017, 2007.

Bitterman Y, Mukamel R, Malach R, Fried I, Nelken I. Ultra-fine frequency tuning revealed in single neurons of human auditory cortex. *Nature* 451: 197–201, 2008.

Bizley JK, Nodal FR, Nelken I, King AJ. Functional organization of ferret auditory cortex. *Cereb Cortex* 15: 1637–1653, 2005.

Blake DT, Merzenich MM. Changes of A1 receptive fields with sound density. *J Neurophysiol* 88: 3409–3420, 2002.

Bregman AS. *Auditory Scene Analysis: the Perceptual Organization of Sound*. Cambridge, MA: MIT Press, 1990.

Brown M, Irvine DRF, Park VN. Perceptual learning on an auditory frequency discrimination task by cats: association with changes in primary auditory cortex. *Cereb Cortex* 14: 952–965, 2004.

Calford MB. The parcellation of the medial geniculate body of the cat defined by the auditory response properties of single units. *J Neurosci* 3: 2350–2364, 1983.

Carlyon RP. The psychophysics of concurrent sound segregation. *Philos Trans R Soc Lond B Biol Sci* 336: 347–355, 1992.

Cheung SW, Bedenbaugh PH, Nagarajan SS, Schreiner CE. Functional organization of squirrel monkey primary auditory cortex: responses to pure tones. *J Neurophysiol* 85: 1732–1749, 2001.

Davis KA, Lomakin O, Pesavento MJ. Response properties of single units in the dorsal nucleus of the lateral lemniscus of decerebrate cats. *J Neurophysiol* 98: 1475–1488, 2007.

Doron NN, Ledoux JE, Semple MN. Redefining the tonotopic core of rat auditory cortex: physiological evidence for a posterior field. *J Comp Neurol* 453: 345–360, 2002.

Edeline JM, Manunta Y, Nodal FR, Bajo VM. Do auditory responses recorded from awake animals reflect the anatomical parcellation of the auditory thalamus? *Hear Res* 131: 135–152, 1999.

Egorova M, Ehret G, Vartanian I, Esser KH. Frequency response areas of neurons in the mouse inferior colliculus. I. Threshold and tuning characteristics. *Exp Brain Res* 140: 145–161, 2001.

Ehret G, Schreiner CE. Frequency resolution and spectral integration (critical band analysis) in single units of the cat primary auditory cortex. *J Comp Physiol A* 181: 635–650, 1997.

Evans EF. The frequency response and other properties of single fibres in the guinea-pig cochlear nerve. *J Physiol* 226: 263–287, 1972.

Gaese BH, Ostwald J. Anesthesia changes frequency tuning of neurons in the rat primary auditory cortex. *J Neurophysiol* 86: 1062–1066, 2001.

Haplea S, Covey E, Casseday JH. Frequency tuning and response latencies at three levels in the brainstem of the echolocating bat, *Eptesicus fuscus*. *J Comp Physiol A* 174: 671–683, 1994.

Harrison RV, Aran JM, Erre JP. AP tuning curves from normal and pathological human and guinea pig cochleas. *J Acoust Soc Am* 69: 1374–1385, 1981.

Kajikawa Y, de la Mothe L, Blumell S, Hackett TA. A comparison of neuron response properties in areas A1 and CM of the marmoset monkey auditory cortex: tones and broadband noise. *J Neurophysiol* 93: 22–34, 2005.

Linden JF, Liu RC, Sahani M, Schreiner CE, Merzenich MM. Spectrotemporal structure of receptive fields in areas A1 and AAF of mouse auditory cortex. *J Neurophysiol* 90: 2660–2675, 2003.

Llano DA, Feng AS. Response characteristics of neurons in the medial geniculate body of the little brown bat to simple and temporally patterned sounds. *J Comp Physiol A* 184: 371–385, 1999.

Lu T, Liang L, Wang X. Neural representations of temporally asymmetric stimuli in the auditory cortex of awake primates. *J Neurophysiol* 85: 2364–2380, 2001.

McLaughlin M, Chabewine JN, van der Heijden M, Joris PX. Comparison of bandwidths in the inferior colliculus and the auditory nerve. II. Measurement using a temporally manipulated stimulus. *J Neurophysiol* 100: 2312–2327, 2008.

Micheyl C, Oxenham AJ. Objective and subjective psychophysical measures of auditory stream integration and segregation. *J Assoc Res Otolaryngol* 11: 709–724, 2010.

Miller LM, Escabi MA, Read HL, Schreiner CE. Spectrotemporal receptive fields in the lemniscal auditory thalamus and cortex. *J Neurophysiol* 87: 516–527, 2002.

Molinari M, Dell'Anna ME, Rausell E, Leggio MG, Hashikawa T, Jones EG. Auditory thalamocortical pathways defined in monkeys by calcium-binding protein immunoreactivity. *J Comp Neurol* 362: 171–194, 1995.

Moshitch D, Las L, Ulanovsky N, Bar-Yosef O, Nelken I. Responses of neurons in primary auditory cortex (A1) to pure tones in the halothane-anesthetized cat. *J Neurophysiol* 95: 3756–3769, 2006.

de la Mothe LA, Blumell S, Kajikawa Y, Hackett TA. Thalamic connections of the auditory cortex in marmoset monkeys: core and medial belt regions. *J Comp Neurol* 496: 72–96, 2006.

Ohl FW, Scheich H. Differential frequency conditioning enhances spectral contrast sensitivity of units in auditory cortex (field AI) of the alert mongolian gerbil. *Eur J Neurosci* 8: 1001–1017, 1996.

Oxenham AJ, Shera CA. Estimates of human cochlear tuning at low levels using forward and simultaneous masking. *J Assoc Res Otolaryngol* 4: 541–554, 2003.

Pelleg-Toiba R, Wollberg Z. Tuning properties of auditory cortex cells in the awake squirrel monkey. *Exp Brain Res* 74: 353–364, 1989.

Philibert B, Beitel RE, Nagarajan SS, Bonham BH, Schreiner CE, Cheung SW. Functional organization and hemispheric comparison of primary auditory cortex in the common marmoset (*Callithrix jacchus*). *J Comp Neurol* 487: 391–406, 2005.

Pickles JO. Psychophysical frequency resolution in the cat as determined by simultaneous masking and its relation to auditory-nerve resolution. *J Acoust Soc Am* 66: 1725–1732, 1979.

Pollak GD, Bodenhamer RD. Specialized characteristics of single units in inferior colliculus of mustache bat: frequency representation, tuning, and discharge patterns. *J Neurophysiol* 46: 605–620, 1981.

Polley DB, Read HL, Storace DA, Merzenich MM. Multiparametric auditory receptive field organization across five cortical fields in the albino rat. *J Neurophysiol* 97: 3621–3638, 2007.

Qin L, Sakai M, Chimoto S, Sato Y. Interaction of excitatory and inhibitory frequency-receptive fields in determining fundamental frequency sensitivity of primary auditory cortex neurons in awake cats. *Cereb Cortex* 14: 13–19, 2005.

Ramachandran R, Davis KA, May BJ. Single-unit responses in the inferior colliculus of decerebrate cats. I. Classification based on frequency response maps. *J Neurophysiol* 82: 152–163, 1999.

Rauschecker JP, Tian B, Pons T, Mishkin M. Serial and parallel processing in rhesus monkey auditory cortex. *J Comp Neurol* 382: 89–103, 1997.

Recanzone GH, Schreiner CE, Merzenich MM. Plasticity in the frequency representation of primary auditory cortex following discrimination training in adult owl monkeys. *J Neurosci* 13: 87–103, 1993.

Recanzone GH, Schreiner CE, Sutter ML, Beitel RE, Merzenich MM. Functional organization of spectral receptive fields in the primary auditory cortex of the owl monkey. *J Comp Neurol* 415: 460–481, 1999.

Recanzone GH, Guard DC, Phan ML. Frequency and intensity response properties of single neurons in the auditory cortex of the behaving macaque monkey. *J Neurophysiol* 83: 2315–2331, 2000.

Rhode WS, Roth GL, Recio-Spinoso A. Response properties of cochlear nucleus neurons in monkeys. *Hear Res* 259: 1–15, 2010.

Ryan A, Miller J. Single unit responses in the inferior colliculus of the awake and performing rhesus monkey. *Exp Brain Res* 32: 389–407, 1978.

Sadagopan S, Wang X. Level invariant representation of sounds by populations of neurons in primary auditory cortex. *J Neurosci* 28: 3415–3426, 2008.

Sadagopan S, Wang X. Contribution of inhibition to stimulus selectivity in primary auditory cortex of awake primates. *J Neurosci* 30: 7314–7325, 2010.

Sally SL, Kelly JB. Organization of auditory cortex in the albino rat: sound frequency. *J Neurophysiol* 59: 1627–1638, 1988.

Suga N. Functional properties of auditory neurones in the cortex of echo-locating bats. *J Physiol* 181: 671–700, 1965.

Suga N, Jen PH. Further studies on the peripheral auditory system of "CF-FM" bats specialized for fine frequency analysis of Doppler-shifted echoes. *J Exp Biol* 69: 207–232, 1977.

Suga N, Tsuzuki K. Inhibition and level-tolerant frequency tuning in the auditory cortex of the mustached bat. *J Neurophysiol* 53: 1109–1145, 1985.

Suga N, Zhang Y, Yan J. Sharpening of frequency tuning by inhibition in the thalamic auditory nucleus of the mustached bat. *J Neurophysiol* 77: 2098–2114, 1997.

Temchin AN, Rich NC, Ruggero MA. Threshold tuning curves of chinchilla auditory-nerve fibers. I. Dependence on characteristic frequency and relation to the magnitudes of cochlear vibrations. *J Neurophysiol* 100: 2889–2898, 2008.

Wu GK, Arbuckle R, Liu BH, Tao HW, Zhang LI. Lateral sharpening of cortical frequency tuning by approximately balanced inhibition. *Neuron* 58: 132–143, 2008.

Zhang H, Kelly JB. Responses of neurons in the rat's ventral nucleus of the lateral lemniscus to monaural and binaural tone bursts. *J Neurophysiol* 95: 2501–2512, 2006.